

Isolation effect analysis on friction pendulum bearings in underground station structures

*Peng Jia¹ and †Zhiyi Chen^{1,2}

¹Department of Geotechnical Engineering, Tongji University, Shanghai 200092, China

²Key Laboratory of Geotechnical and Underground Engineering of Ministry of Education, Shanghai 200092, China

*Presenting author: 919526724@qq.com

†Corresponding author: zhiyichen@tongji.edu.cn

Abstract

The previous earthquake surveys show that the central columns are the weak parts in subway stations during the earthquakes. Reducing the seismic responses of the central columns can ensure the safety of the stations. Setting friction pendulum bearings at the top of the central columns may be a good strategy. In this paper, based on a subway station in Shanghai, the friction pendulum bearings is simulated detailedly and the isolation effect of the friction pendulum bearings is studied with the three-dimensional dynamic time history analysis method. The results show that the friction pendulum bearings can effectively reduce the shearing force of the central columns and slightly reduce the bending moment during the earthquake. At the same time, they does not cause a significant increase in deformation of the side walls. It is stated that the friction pendulum bearings are also effective in the underground station structures.

Keywords: Underground subway station, Friction pendulum bearings, Seismic Response

1. Introduction

In 1987, Zayas et al. developed a friction pendulum bearing at the University of California, Berkeley [1]. At present, more than 10 kinds of friction pendulum bearings have been developed. The most common friction pendulum bearing is the single curved surface friction pendulum bearing, which is mainly composed of a slider, a lower base and an upper base.

Friction pendulum bearings have been widely used in above-ground structures, but rarely in underground structures [2][3]. Since the Kobe earthquake in Japan caused severe damage to the Dakai Station in 1995, the seismic capacity of underground structures has gotten more and more attention. Previous studies have shown that the damage of the underground station structure is mainly caused by the damage of the central columns [4]. Strengthening the seismic performance of the central columns can effectively improve the seismic capacity of the underground station. Setting friction pendulum bearings at the top of the central columns may be a good strategy.

2. Fine simulation of FPB

At present, the most common friction pendulum bearing on the ground is the single curved friction pendulum bearing. It is mainly composed of three parts, which are an upper base, a lower base and a slider. During the earthquake, the slider is mainly subjected to the vertical pressure, horizontal force transmitted by the structure, support force and friction on the concave surface. According to the force's equilibrium condition, Eq. (1) can be get that:

$$F = \frac{WD}{R \cos \theta} + \frac{f}{\cos \theta} \quad (1)$$

When the angle of rotation is relatively small, it can be approximately simplified as Eq. (2).

$$F = \frac{WD}{R} + f = \frac{WD}{R} + \mu W \operatorname{sgn}(\dot{\theta}) \quad (2)$$

where, F is horizontal force transmitted by the structure, W is vertical pressure, R is the radius of the concave surface, D is the relative displacement of the slider, and μ is the friction coefficient of the sliding surface [5].

The ABAQUS finite element software is used to carry out the refined simulation [6]. The finite element model of the friction pendulum bearing is shown in Figure 1. The concave radius is 2m and the friction coefficient of the sliding surface is 0.1.

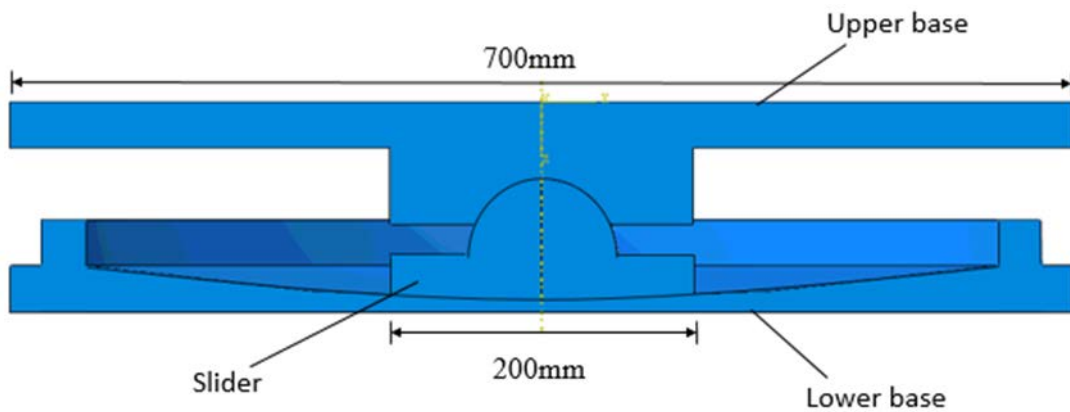


Figure 1. Fine simulation of FPB

Applying a vertical pressure of 2000kN to the friction pendulum bearing. The force-displacement curve of the finite element model is compared with the result calculated by the Eq. (2). As shown in Figure 2, the two curves are roughly coincident, indicating that the refined finite element model can simulate the mechanical characteristics of the friction pendulum bearing well.

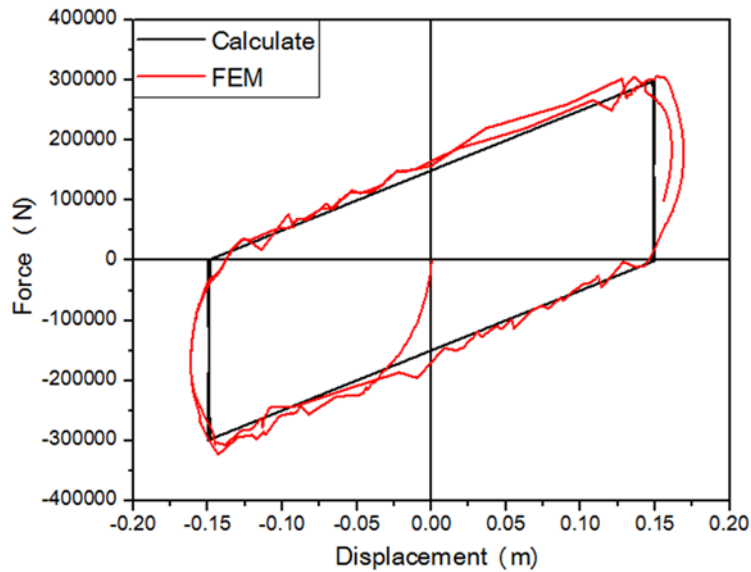


Figure 2. The force-displacement curve of FPB

3. Numerical Simulation

3.1 Finite element model

A cross section of the station is shown in Figure 3. The station is 21.84m wide and 13.1m high. The cross section dimensions of the upper and lower central columns are both 0.7m×0.7m, and the interval between the central columns is 5.8m.

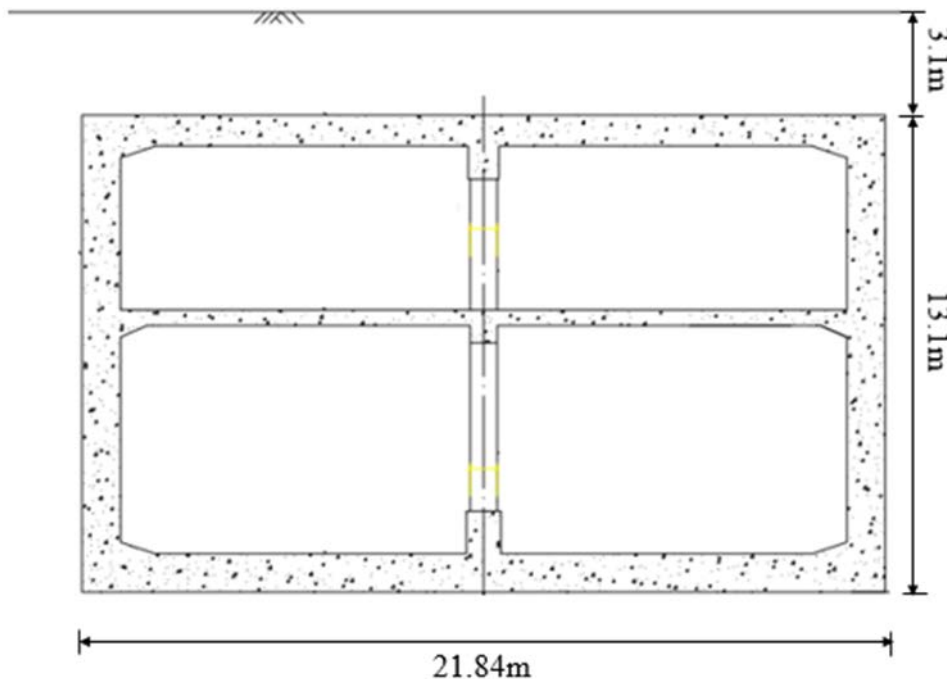


Figure 3. The cross section of the station

The ABAQUS finite element software was used to establish a three-dimensional finite element model of the station and soil layers. The dimensions of the station model are established according to the cross section shown in Figure 3. According to the detailed geotechnical survey report of the project, the soil can be divided into ten layers. The thickness

and basic physical properties of each layer are shown in Table 1. The overall size of the model is 80m long, 60m high and 5.8m wide, since the interval between the central columns in the station is 5.8m, as shown in Figure 4.

Table 1. The basic physical properties of each soil layer

Soil number	Soil texture	Thickness (m)	Density (g/m ³)	Internal friction angle(°)	Cohesion (kPa)
1	Artificial fill	1.3	1900	15	20
2-1	Yellowish dark brown silty clay	1.1	1920	31.3	9.5
2-2	Yellow gray silty clay	1.1	1800	33.8	15.1
3	Gray mucky silty clay	3.4	1740	28.3	5.3
4	Gray mucky clay	8.2	1670	24.9	7.2
5-1	Gray clay	1.6	1740	29.7	10
6	Dark green silty clay	4.4	1950	29.1	31.3
7	Olive drag-gray sandy silt	6.9	1820	31.1	2
8-1	Gray clay	15	1770	32.5	8.1
8-2	Gray silty clay and silty sand interbedded soil	17	1840	28.1	8

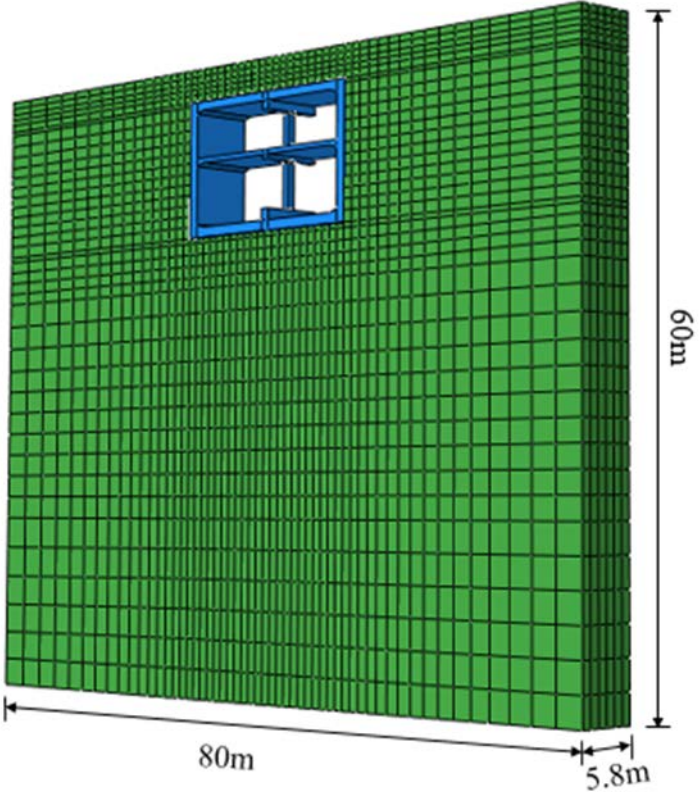


Figure 4. The finite element model of the station and soil

The boundary conditions of the ground are fixed at the bottom, and an equal displacement boundary is adopted to the four side boundaries, so that each layer elements have the same horizontal displacement. The equal displacement constraint can avoid the reflection of seismic

waves at the boundary [7][8].

3.2 Constitutive models

The station is a reinforced concrete structure. To simplify the analysis, the material is equivalent to a homogeneous material, and the material parameters are approximated to the concrete's. The density of the material is 2500kg/m³, the Poisson's ratio is 0.2, and the modulus of elasticity is 31.5Gpa.

In order to simulate the dynamic properties of the soil, an equivalent linear viscoelastic model with damping is used. The dynamic elastic modulus of the soil layers can be calculated according to the Eq. (3)

$$G = \rho V_s^2$$

$$E = 2(1 + \sigma)G \quad (3)$$

where, V_s is the shear wave velocity, ρ is the soil density, σ is the Poisson's ratio, and G is the equivalent dynamic shear modulus of the soil. The variation of the shear wave velocity along the depth is in accordance with the law of exponential or logarithm. For the Shanghai region, the exponential form can be selected, as shown in Eq.(4).

$$V_s = aH^b \quad (4)$$

where, H is the depth of soil layers, a and b are the calculation parameters. For the area where the station is located, a and b are 79.03 and 0.3437 [9]. The soil layer parameters obtained by calculation are shown in Table 2.

Table 2. The parameters of each soil layer

Soil number	Depth (m)	Shear wave velocity (m/s)	Shear modulus (Gpa)	Poisson's ratio	Elastic modulus (Gpa)
1	1.3	86	14.2	0.32	37.5
2-1	2.4	107	21.9	0.32	57.8
2-2	3.5	122	26.6	0.34	71.3
3	6.9	153	41	0.38	113.2
4	15.1	201	67.4	0.4	188.8
5-1	16.7	208	75.2	0.35	203.2
6	21.1	225	99.1	0.29	255.6
7	28	248	112.3	0.29	289.8
8-1	43	288	146.7	0.33	390.2
8-2	60	323	191.7	0.32	506.2

The damping of the soil is Rayleigh damping. Using the modal analysis function of ABAQUS, the first-order mode frequency of the site is 0.36Hz, and the second-order mode frequency is 1.08Hz. Rayleigh damping coefficient can be calculated according to the Eq. (5).

$$\xi = \frac{\alpha}{2} \times \frac{1}{\omega_1} + \frac{\beta}{2} \times \omega_2 \quad (5)$$

where, ω_1 and ω_2 are the main mode frequencies of the soil, and the damping ratio ξ is 0.05. It is calculated that the Rayleigh damping coefficient $\alpha = 0.1698$, $\beta = 0.0129$.

3.3 Ground motion characteristics

In order to study the seismic response of the station, the seismic waves are input in the Y direction at the bottom of the model. The Shanghai artificial wave is selected as the input ground motion. The acceleration time history curve and the Fourier spectrum of the seismic wave are shown in the Figure4.

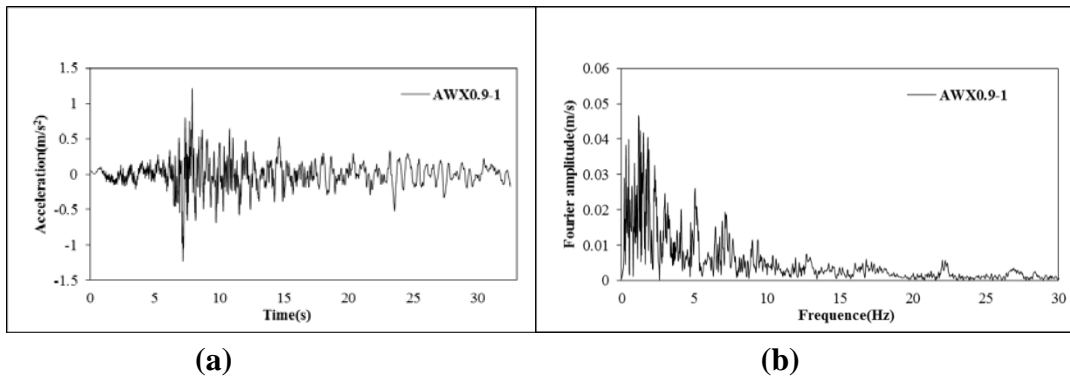
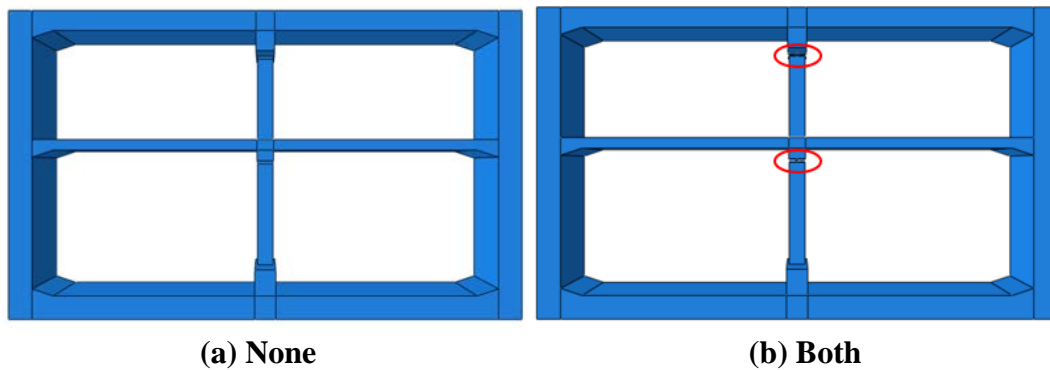


Figure 4. Shanghai artificial wave characteristics: (a) Acceleration time history curve and (b) Fourier spectrum

3.4 Cases introduction

As the station is a frame structure with two floors and two spans, the friction pendulum bearings are placed on the top of the central columns, so there are four arrangements, as shown in figure5. That is, the friction pendulum bearings are not arranged, the friction pendulum bearings are arranged in both floors, the friction pendulum bearings are arranged only on the upper floor and the friction pendulum bearings are arranged only on the lower floor. And the amplitude of seismic wave acceleration is 0.1g and 0.5g.



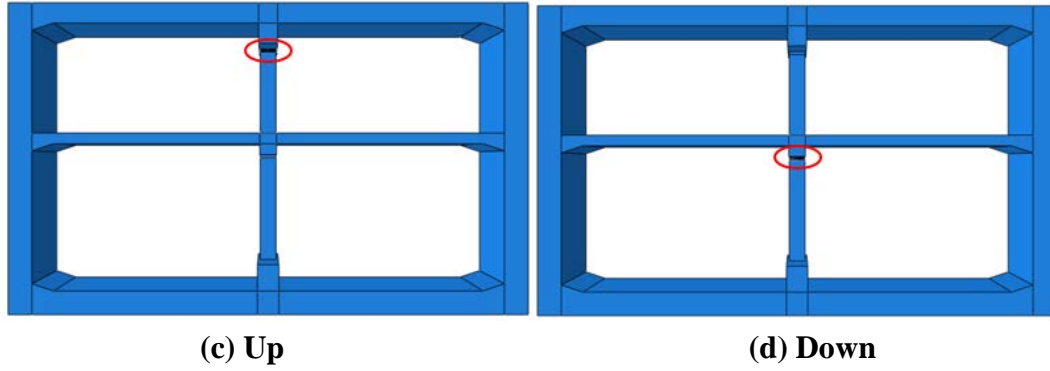


Figure 5. Four different arrangements: (a) FPB are not arranged, (b) FPB are arranged in both floors, (c) FPB are arranged in upper floor, (d) FPB are arranged in lower floor

4. Isolation effect of friction pendulum bearings

4.1 Seismic response of the central columns

The destruction of the underground stations is mainly caused by the destruction of the central columns. The bending and shearing is the major failure form of the central columns. So the maximum bending moment and shearing force at the bottom of central columns are extracted as the indexes of dynamic response during the earthquake. In different cases, the shearing force at the bottom of the central columns in two floors is shown in Table 3.

Table 3. The shearing force in central columns in different cases

Case	0.1g		0.5g	
	Lower floor (kN)	Upper floor (kN)	Lower floor (kN)	Upper floor (kN)
none	178	213	854	1105
both	87	110	427	390
up	187	81	911	366
down	88	257	429	1307

The isolation effect of friction pendulum bearings is defined as Eq. (6)

$$\gamma = (R_0 - R_f) / R_0 \quad (6)$$

where, R_f is dynamic response of central columns with friction pendulum bearings and R_0 is the response without friction pendulum bearings. In each case, the isolation effect on the shearing force of the central columns is shown in the Table.4 and Figure 6.

Table 4. The isolation effect on shearing force in central columns in different cases

Case	0.1g		0.5g	
	Lower floor	Upper floor	Lower floor	Upper floor
none	-	-	-	-
both	51.1%	48.4%	50.0%	64.7%
up	-	62.2%	-	66.9%
down	50.4%	-	49.8%	-

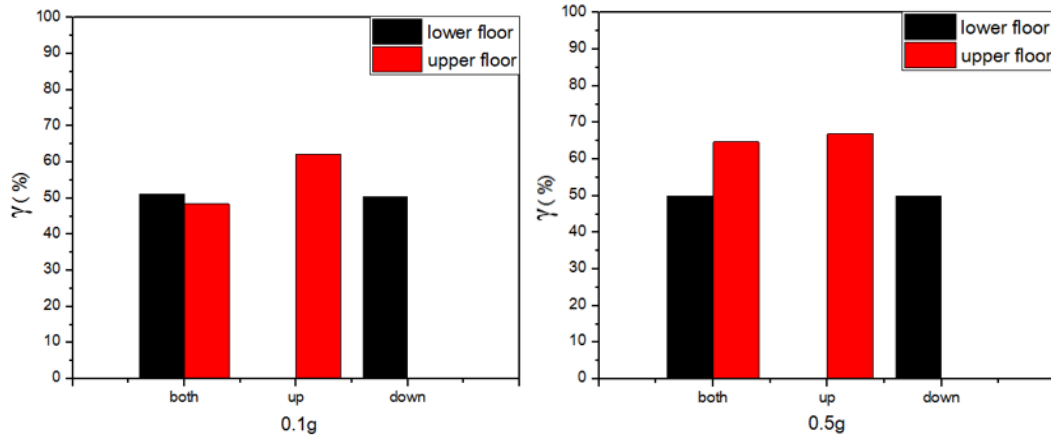


Figure 6. The isolation effect on shearing force in central columns in different cases

It can be found from the results that the friction pendulum bearings can effectively reduce the maximum shearing force on the central columns during the earthquake. When the friction pendulum bearings are placed on one of the two floors, the maximum shearing force during the earthquake in the central columns of this floor is significantly reduced. The maximum shearing force in the other floor's central columns is slightly increased. And in different cases, the bending moment at the bottom of the central columns in two floors is shown in Table 5.

Table 5. The bending moment in central columns in different cases

Case	0.1g		0.5g	
	Lower floor (kN*m)	Upper floor (kN*m)	Lower floor (kN*m)	Upper floor (kN*m)
none	360	275	1780	1322
both	295	260	1427	1046
up	369	220	1840	990
down	299	374	1450	1787

In each case, the isolation effect of the isolation bearing on the bending moment of the central columns is shown in the Table 6 and Figure7.

Table 6. The isolation effect on bending moment in central columns in different cases

Case	0.1g		0.5g	
	Lower floor	Upper floor	Lower floor	Upper floor
none	-	-	-	-
both	18.1%	5.5%	19.8%	20.9%
up	-	20.0%	-	25.2%
down	17.0%	-	18.6%	-

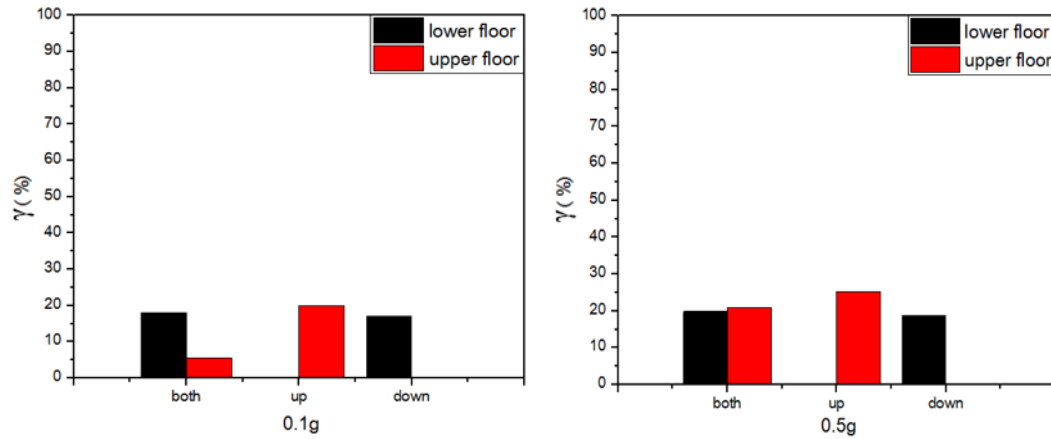


Figure 7. The isolation effect on bending moment in central columns in different cases

It can be found from the results that the friction pendulum bearings can reduce the maximum bending moment on the central columns during the earthquake. The isolation effect on the bending moment is not obvious compared with the shearing force. When the friction pendulum bearings are placed on one of the two floors, the maximum bending moment in the other floor's central columns is slightly increased.

4.2 Seismic response of the side walls

The station studied in this paper is a two-story and two-span frame structure. The deformation of the side walls during the earthquake can be judged by inter-layer displacement and inter-layer displacement angle. In different cases, the inter-layer displacement and inter-layer displacement angle are shown in Table 7 and Table 8.

Table 7. The inter-layer displacement in different cases

Case	0.1g		0.5g	
	Lower floor (mm)	Upper floor (mm)	Lower floor (mm)	Upper floor (mm)
none	5.16	3.41	25.38	17.56
both	5.26	3.49	26.11	17.72
up	5.17	3.53	25.43	18.12
down	5.22	3.37	25.81	17.23

Table 8. The inter-layer displacement angle in different cases

Case	0.1g		0.5g	
	Lower floor	Upper floor	Lower floor	Upper floor
none	1/1198	1/1488	1/243	1/289
both	1/1176	1/1452	1/237	1/286
up	1/1194	1/1436	1/243	1/280
down	1/1183	1/1505	1/239	1/294

In each case, compared with the station without friction pendulum bearings, the percentage increment of the inter-layer displacement and the inter-layer displacement angle after the friction pendulum bearings are set is shown in the Table 9.

Table 9. The percentage increment of the inter-layer displacement

Case	0.1g		0.5g	
	Lower floor	Upper floor	Lower floor	Upper floor
none	-	-	-	-
both	1.9%	2.5%	2.8%	0.9%
up	-	3.6%	-	3.2%
down	1.2%	-	1.7%	-

It can be found from Table 9 that the friction pendulum bearings can effectively reduce the shearing force and slightly reduce the bending moment of the central columns. And they will only increase the interlayer displacement and the interlayer displacement angle by 1-4%. That is, they will not cause a significant increase in the internal force and deformation of the side wall.

5. Conclusion

In this paper, through the refined finite element model, the isolation effect of the friction pendulum bearings in the underground structure is studied, and the following conclusions are obtained.

- (1) The friction pendulum bearings can effectively reduce the shearing force received by the central columns in the station, and the reduction can exceed 60%.
- (2) The friction pendulum bearings effectively reduce the shearing force of the central columns in the station, but the isolation effect on the bending moment is not obvious.
- (3) The reduction of the internal force of the central columns on which the friction pendulum bearings are arranged does not cause a significant increase in the deformation of the side walls.

This paper proves that friction pendulum bearing is also effective in the underground station. And they can significantly improve the stations' earthquake resistance

References

- [1] Zayas V, Low S and Mahin S. The FPS earthquake resisting system. (1987) Technical Report UCB/EERC-87 /01, University of California at Berkeley.
- [2] Paolo M. Calvi, Gian Michele Calvi. (2018) Historical development of friction-based seismic isolation systems. *Soil Dynamics and Earthquake Engineering* **106**, 14-30.
- [3] P. Scott Harvey Jr., Karah C. Kelly. (2016) A review of rolling-type seismic isolation: Historical development and future directions. *Engineering Structures* **125**, 521-531.
- [4] Chao Ma, De-Chun Lu, Xiu-Li Du, Cheng-Zhi Qi, Xiang-Yang Zhang. (2019) Structural components functionalities and failure mechanism of rectangular underground structures during earthquakes. *Soil Dynamics and Earthquake Engineering* **119**, 265-280.
- [5] P. Castaldo, B. Palazzo, P. Della Vecchia. (2015) Seismic reliability of base-isolated structures with friction pendulum bearings. *Engineering Structures* **95**, 80-93.
- [6] ABAQUS. Standard User's Manual, vols. I & II. (2009) Hibbit, Karlsson & Sorensen Inc. Pawtucket, Rhode Island.
- [7] A. E. Kampitsis, E. J. Sapountzakis, S. K. Giannakos, N. A. Gerolymos. (2013) Seismic soil–pile–structure kinematic and inertial interaction—A new beam approach. *Soil Dynamics and Earthquake Engineering* **55**, 211-224.
- [8] A. M. MARSHALL, R. FARRELL, A. KLAR, R. MAIR. (2012) Tunnels in sands: the effect of size, depth and volume loss on greenfield displacements. *Geotechnique* **62(5)**, 385-399.
- [9] Fei Gao, Xiaogang Sun. (2005) Characteristics analysis of shear wave velocity of foundation ground in Shanghai region. *Shanghai Geology* **2**, 27-29.